ISSN (Print) : 0974-6846
Indian Journal of Science and Technology, *Vol 8(17), DOI: 10.17485/ijst/2015/v8i17/70181, August 2015* ISSN (Online) : 0974-5645

Stability Enhancement of Doubly Fed Induction Generator with Virtual Resistance for Grid Disturbances

Krishna Manjusha Kondapi* **and R. B. R. Prakash**

Department of Electrical and Electronics Engineering, KL University, Vaddeswaram, Guntur District-522502, Andhra Pradesh, India; manjusha.kondapi@ymail.com

Abstract

In a doubly fed induction generator the rotor is connected to the grid through the AC/DC/AC rotor converters. When a fault occurs in the grid, abnormal currents will be circulating in the rotor and rotor side converters. In olden days the grid stability maintained by crowbars but this method has few considerable limitations.In this paper virtual resistance is proposed to protect the rotor side converters increases the stability of the system. In keeping the requirements of the reactive power in wind farms, crowbars are not preferable they absorb the reactive power from grid whereas by virtual resistance system supplies the reactive power to the grid. In order to regulate the virtual resistance PI method and Fuzzy logic controller method are developed, outputs are compared. By using virtual resistance system stability is enhanced as the rotor demagnetizing currents are developed to cut off the dc and negative flux of the stator. The concept of virtual resistance for stabilizing the system during grid faults is opted by using a fuzzy logic controller the total harmonic distortion is reduced which are observed in the output waveform compared to PI controller.

Keywords: Crowbars, Doubly Fed Induction Generator, Virtual Resistance

1. Introduction

Development in power generation by Wind energy is briskly rising every year due to its advantages. It doesn't produces greenhouse gases, occupies less area on land and its maintenance is also very low. DFIG is used for more than one megawatt power generation as it has dominance on wavering speed and fixed frequency, decoupled managing of active and reactive power the rotor power is controlled by converters. It has many cons like less in size, weight, and in cost, low losses correlated with directly drive wind power generators having a power converter. In wind farms, the stator of DFIG is precisely connected to the grid so it is highly conscious to the faults occurred in grid. Voltage gets decreased at stator when a disturbance occur in grid, therefore rotor cause high voltages which damages the converters connected to rotor and high voltage disturbances occurs in the system. High rotor inflow current, dc overvoltage and torque oscillations results damage of the doubly fed induction generator[1-4]this results the failure of rotor converters and mechanical parts. Previously whenever high currents occur in rotor windings a circuit namely crowbars are worn to look after the rotor converter, it short circuits the winding of rotor. Figure 1 is shows the crow bar circuit in DFIG construction of wind power system[5-7]. It consists of resistor supervised by power electronic devices. There is need to know the grid code values and fault ride through capabilities of the turbine.

An international standard so called E.ON standards shows grid code whose LVRT capacity is shown in Figure 2 Wind turbines can be kept running if the voltage is

* *Author for correspondence*

0.15pu for 0.625 seconds. If else it downs lower that value and gains 90% of its ostensible voltage value in less than 3 seconds immediate when voltage decreases the turbine can run normally

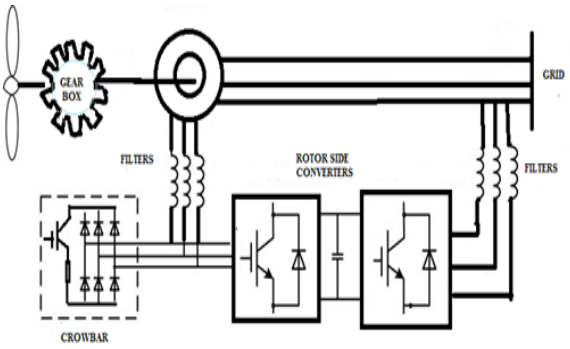

Figure 1. DFIG Connected with Crow- bars.

Active power output regains when fault was cleared and reactive power should give back to the grid below 20ms when fault was analyzed[8,9].

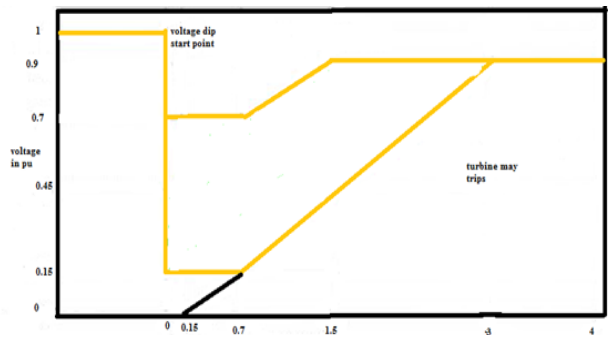

Figure 2. E.ON.Grid Voltage Standards.

Crowbars care the rotor converters but it converts doubly fed induction generator to squirrel cage induction generator, it consumes high reactive power from the grid. Due to this action voltage at grid falls drastically. So turbine with crow bar is not efficient in maintaining grid codes, there is another disadvantage like equipment cost and it not decisive. To fulfill the new grid codes LVRT capacity is crucial for DFIG. Many researchers have brought techniques to control this rather than using a crowbar[6,10,11].As crowbar has pros it is replaced with static synchronous compensator which gives reactive power when connected at terminal[12,13], these are high in cost, many such proposals are done[14-18], here the aim of the paper is to control the DFIG at high currents in windings of rotor when faults occur in grid, by using virtual resistance in the system, demagnetizing currents are developed to cut off the dc and negative flux of the stator. Whole system is controlled by the virtual resistance and demagnetization control.

2. Modeling of Doubly Fed Induction Generator in Voltage Sag

2.1 Mathematical Modeling of Doubly Fed Induction

From Park model[7,19] which is need to evaluate the behaviorof the DFIG. Park model[7,19] is usually used to analyze the behavior of the DFIG. Voltages of stator and rotor are expressed as follows.

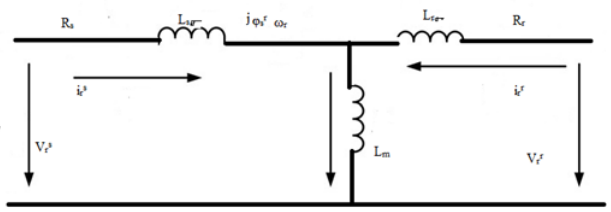

Figure 3. Park Model Circuit of DFIG.

where "r" indicates rotor frame reference "s" as stator frame v_r^s and v_r^r are voltages, i_r^s and i_r^r are currents, R_s and R_r are resistances, ω_r is rotors angular velocity, ψ_r^s and ψ_r^r are fluxes. The stator and rotor fluxes are expressed as

$$V_r^r = R_s I_s^r + j\omega_r \varphi_r^r + d\varphi_r^r / dt \quad (2.1)$$

$$V_r^r = R_r I_r^r + \quad + d\varphi_r^r / dt \quad (2.2)$$

L_s and L_r indicates self-inductances, $L_{\sigma r}$ and $L_{\sigma s}$ are rotor and stator leakage inductances, L_m is the mutual inductance between the stator and rotor. The rotor flux is gained from with (2.3) and (2.4)

$$\psi_r^s = L_s i_s^r + L_m i_r^r \quad (2.3)$$

$$\psi_r^r = L_m i_s^r + L_r i_r^r \quad (2.4)$$

$$\psi_r^r = L_m / L_s * \varphi_s^r + \sigma L_r I_r^r \quad (2.5)$$

so the equivalent DFIG model from a rotor side[6, 7, 15, 19] is gained and shown in Figure 4, E represents EMF induced by a stator flux, is shown below, from Figure 4, the rotor current is observed from injected rotor voltage and emf is the derivative of stator flux linkage.

$$E = L_m / L_s * d / dt\varphi_s^r \quad 2.6$$

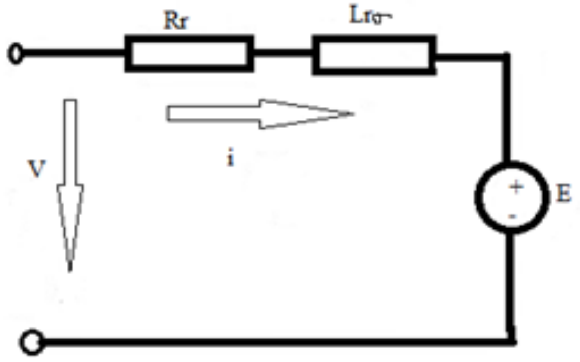

Figure 4. Equivalent DFIG.

2.2 Behavior of Doubly Fed Induction Generator under Grid voltage Gags

Taking stator reference frame, the space vector voltage of stator v_s^s is shown as

$$V_s^s = Rsi_s^s + d / dt\varphi_s^s \quad 2.7$$

Where subscript "s" shows equation in the stator reference frame, V_s^s, i_s^s and ψ_s^s indicates the stator voltage, current, and flux space vector. Considering faults in the grid, by symmetrical component theory[7,15], the voltage of stator is of three parts- positive, negative and zero sequence component, the zero sequence components is zero as DFIG is connected to grid, it can be written as

$$V_s^s = Vpe^{j\omega st} + Vne^{-j\omega st} \quad 2.8$$

Vp and Vn are amplitude of positive and negative sequence components. The stator voltage during symmetrical and asymmetrical sags are simultaneously shown in (2.8)

During symmetrical sag, the negative sequence in (2.8) is neglected. If Rs is kept zero, from (2.7) and (2.8) flux at faults is shown

$$\psi_{ss}^s = Vpe^{j\omega st} / j\omega s + V_n e^{-j\omega st} / -j\omega s \quad 2.9$$

$$\psi_{ss}^s = \text{stator flux steady} - \text{state component}$$

By circuit theory, the flux is a state variable it doesn't lose continuity and it differs from its beginning state to its steady state, the transient component and steady-state component at grid voltage sag of flux is,

$$\psi_{ss} = \psi_{ss}^s + \psi_{st}^s + V_p e^{j\omega st} / j\omega s + V_n e^{-js\omega t} / -j\omega s + \varphi_{st} e^{-t/\tau} \quad 2.10$$

ψ_{st}^s and φ_{st} = transient component of the stator flux and its initial value, whereas τ represents time constant.

$$E = L_m / L_s s V_p e^{js\omega st} + L_m / L_s (s-2) V_n e^{-j(2-s)\omega st} + L_m / L_s (1-s) C e^{-t/\tau ej\omega rt} \quad 2.11$$

C = simplified coefficient, from (2.11), E has three parts: positive, negative, and dc components of the stator flux, where s is low value which exists between −0.3 to +0.3, the other two parts generated by negative and dc components of the stator flux in grid faults can result high voltages and currents at rotor side. In normal condition, positive component exists , the other two terms in (2.11) are neglected, the generated stator flux has synchronous peed, at rotor winding, the flux rotate at the slip speed which is shown in (2.11), high voltages or currents doesn't appear , so rotor converter doesn't get destroyed at normal condition and vice versa. Voltage dips at grid are of two types symmetric dip and asymmetric dip, when dip is symmetric, negative component is zero, aggressive ruined component of dc and positive sequence component will present were identified from voltage of stator subsequently when dip occur, 3rd term in (2.11), the EMF component is corresponding to (1−s) which is developed by dc component, is greater than the EMF developed at regular condition (s) furthermore, from 1stterm in (2.11), the EMF is generated by a positive components and slip rate s are proportional to each other, hence EMF is higher than in regular condition. Considering the asymmetric dip situation, the stator flux has an aggressively ruined dc component, positive component, and negative component, are shown in (2.11), where the total EMF has 3 terms, the negative flux component with speed $-\omega_s$ and at speed $(s-2)\omega_s$ with respect to rotor, as slip is very low small and frequency is doubled. Taking the 2nd term in (2.11), the EMF generated by a negative flux component and (s−2) are proportional, hence the total EMF at asymmetric dip is very high compared to normal conditions, like-wise the severe voltage dip at gridgenerated EMF cross the peak voltage of the rotor converter resulting the high rotor current causing drastic voltage increment[6, 2-8, 20], the high inflow currents occurs at rotor circuit, when currents reaches the peak value that if the rotor converter can manage, the Rotor side converters gets heavily destroyed . During a dip which is asymmetrical, a crowbar is implemented to safe

guard the rotor converters, it should be in running till the dip disappears, this leads generator to take high reactive power from grid causing high voltage dip and can't reach grid code values

3. Proposed Techniques

Research on LVRT is compensated by stator flux with a converter connected in series to[14-16] or By circuit theory, the flux is a state variable it doesn't lose continuity and it changes from its starting state to its steady state, hence rotor current control scheme is developed[6,17,21]. This has disadvantages like its price and size in the system. Author named Xiang et al. proposed a rotor current control scheme in[17], one author Lopez et al.[6,2] presented a paper on demagnetizing currents and the crowbar. Even though the drawback still exist as the demagnetizing current depends on DFIG parameters.

3.1 Proposal of Virtual Resistance

Equivalent diagram of DFIG model in Figure 4, the inner current loop of the DFIG is shown in Figure 5. Where C(s) = transfer function of current regulator, A(s) = transfer function of the rotor converter, G(s) = transfer function of the DFIG according to inner current loop which is shown in[8, 22].

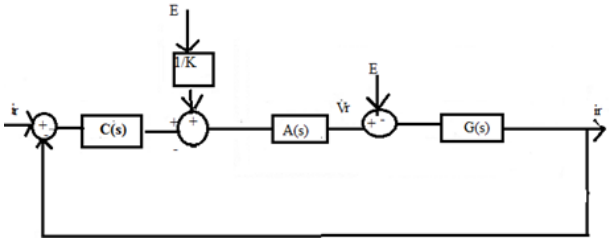

Figure 5. DFIG control block with inner current loop.

$$G(s) = 1/R_r + \sigma L_r s \quad 3.1$$

Where K = converter gain. As shown in Figure 5, E represents disturb term effects the dynamics of inner current loop of the crowbar to maintain the impact on E, partial feedback is worn for reduction of time constant to raise the dynamic characteristics , the control block with limited feed- back is shown in Figure 6[23,24]. F(s) = partial feedback transfer function, expecting that F(s) is a proportional feedback then F(s) = R_f, where the delay of the converter is negotiated, simplifying A(s) as K, the transfer function is represented in in Figure 6 equation with partial feed back

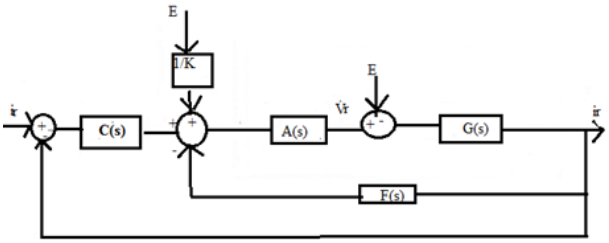

Figure 6. DFIG Control Block with Partial Feedback Inner Current Loop.

$$Go(s) = K\,R_r + \sigma L_r s \quad 3.2$$

$$Go'(s) = K/(Rr + K\ \ Rf) + \sigma Lr \quad 3.3$$

Comparing (3.2) with (3.4), the sectional feedback is equal to the series resistor of the DFIG and the value of the rotor resistor is KR_f , by taking the equivalent model of DFIG from Figure 3 and Figure 3 with a sectional feedback is shown in Figure 7. Implementing a resistor in series to the rotor of DFIG in Figure 7 is used to reduce the impact of EMF on currents of the rotor.

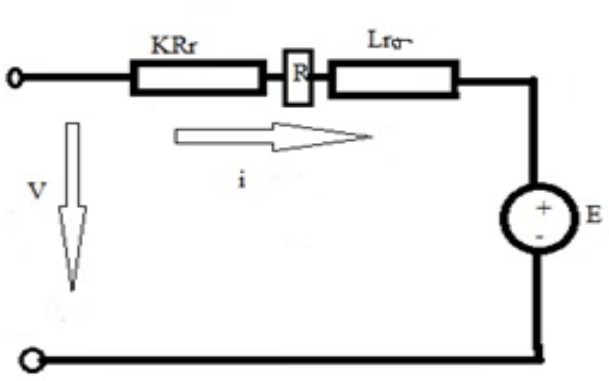

Figure 7. Equivalent DFIG with Resistance Partial Feed back.

This resistor is named as "virtual resistor" it can't be seen, like wise a virtual inductance can also be implemented if feedback transfer F(s) = Lf s, therefore the objective transfer function with virtual resistor and virtual inductance can be expressed as

$$Go'(s) = K/(Rr + K\ \ Rf) + (\sigma L_r + K\ \ Lf)s \quad 3.4$$

Certainly to boycott the noise an inductance is used which is shown in (3.5)

$$L(s) = L_f s/T_s + 1 \quad 3.5$$

T = Low-Pass Filter (LPF). By changing equation (3.5) into z-domain with backward differential method,

s =(1-z-1)/Ts, is determined as

$$L(z) = L_f - L_f z^{-1} / (T + T_s) - T z^{-1} \quad 3.6$$

Ts = sampling period. In this system, the sampling frequency is 5.4 kHz and corner frequency of LPF is 1 kHz. By implementing virtual resistance and inductance it reduces rotor current generated by EMF at grid faults and the rotor and leakage inductances of stator of the DFIG is low with virtual resistance, time of oscillation can also be reduced. With this the LVRT for the DFIG is enhanced.

$$Go(s) = K_1 / 1 + T_1 s \quad 3.7$$

where $K_1 = K/R_r$, $T_1 = \sigma L_r / R_r$, let K_1 changes with ΔK_1 because of change in machine parameter, K_1 is $K_1 + \Delta K_1$ in (3.7) hence the change is $\Delta K_1 / K_1$ because of change in machine parameter, by implementation of a virtual resistance with a feedback. The transfer function (3.7) is derived as

$$Go'(s) = K1'/1 + T1's \quad 3.8$$

Where $K_{1'} = K_{1'} (1 + R_f K_1)$, $T_{1'} = T_{1'} (1 + R_f K_{1'})$, similarly if $K_{1'}$ changes with $\Delta K_{1'}$ becauseof change in machine parameter, $K_{1'}$ changes to $\Delta K_{1'}$ it is written as

$$\Delta K_{1'} = \partial K_{1'} / \partial K_1 \Delta K_1 = \Delta K_1 (1 + R_f K_1)^2 \quad 3.9$$

Hence with feedback control, change can be expressed as

$$\Delta K_{1'} = K_1 (1 + R_f K_1) \times \Delta K_1 K_1 \quad 3.10$$

From (3.10), with virtual resistance, the impact of machine parameter changes on a system is reduced by $1/(1+R_f K_1)$ times.

4. Control Strategy

The enhanced control strategy is introduced to decrease the currents of rotor at grid during a voltage dip, the developed control technique is having a regular vector controller, low voltage ride through technique controller, and reactive power mathematical model, voltage dip detection and switching control module Magnetization controlling scheme was introduced in[6], that build on the components of the DFIG[17,18], where the leakage of the DFIG is very low, current of the rotor is high at voltage dip. The idea of the LVRT controller in the present control Strategy consists of demagnetization control and virtual resistance control, as expected the implementation of virtual resistance will reduce the rotor current and its decayed time

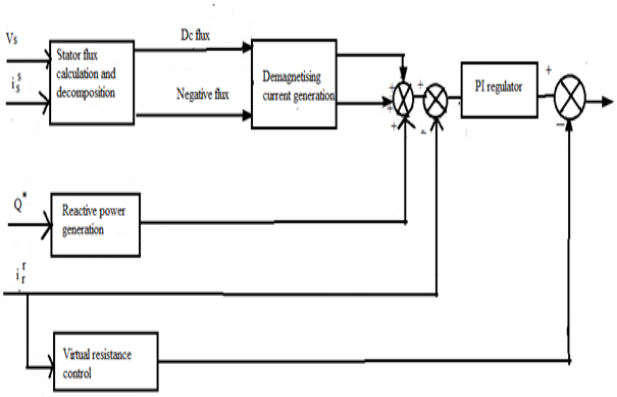

Figure 8. LVRT Controller.

Current also gets reduced, the usage of crowbar is not necessary. Giving reactive power to the grid helps in the voltage gain at voltage sag[25,26], but in this technique, reactive power is given to the grid with respect to the intensity of dip Figure 8 indicates the developed LVRT controller containing a control block of demagnetization, virtual resistance andreactive power generation block

4.1 Grid Fault Identification

In switching normal controller to the LVRT controller, quick detection of fault at grid is important[27]. The voltage dips are of two types,symmetric dip and asymmetric dip, symmetric dip contains a positive component in the stator voltage so the wind generator system is a 3-line and 3-Φ system and the detection of voltage dip at symmetric dip can detected by converting 3-Φ voltage variables in a common reference frame to a synchronous d-q reference frame. The converted d-q variables are corresponding to the magnitude of the stator voltage, so comparing with the values of d-q variables when voltage dip is zero and with voltage dip, voltage dip can be detected. Similarly in asymmetric sag it consists of positive component and negative components in the stator voltage, the new d-q variables consists a second order ac harmonic component with a dc component. To get the dc component, one technique is to utilize LPF to remove the harmonic component; when positive component in d-q reference frame was identified, the detection method is similar to that of a symmetric dip. In technique of converting the 3-Φ variables to αβ

reference frame, the positive sequence variable is existed by the quarter cycle delayed algorithm.

5. Simulation and Results

In order to calculate the ride through capability by proposed technique, the system wassimulated with 100% voltage sags, virtual resistance is considered at a peak value, current source is not connected in series with inductive for normal working condition the capacitance value is $1e^{-6}$ F where impedance reactive model can be neglected, before dip DFIG operates at super synchronous mode, where rotor current and voltage with demagnetizing control is observed. Rotor current is lesser than the normal value. Stator current is doubled, slip normally exists between -0.3 to +0.3.rotor voltage is kept in control not exceeding the rated value. Of course the voltage of the rotor by using virtual resistance is greater than the demagnetizing control or at maximum dip.by giving reactive power to grid it maintains the voltage at grid and grid code values are kept maintained so the rotor current is at normal value protecting the converters without the usage of any crowbar or power electronic equipment's. The stator currents are also controlled, so virtual resistance decreases the cost n price. We considered fault at 0.38sec we can observe the torque drop at 0.38 sec under fault condition and regains to its normal value after fault cleared shown in Figure 9. The speed of the rotor also reduces at a particular instant where fault was identified and comes to its normal value shown in Figure 9. The stator and rotor currents gets fluctuated at fault condition and reaches to the nominal value after fault was cleared is shown in Figure 10, that stator and rotor Currents rise to maximum points. The fault at 0.38 sec occurs in line and ground where the voltage dips are seen in Figure 11. The dq to abc transformation is seen in Figure 12.

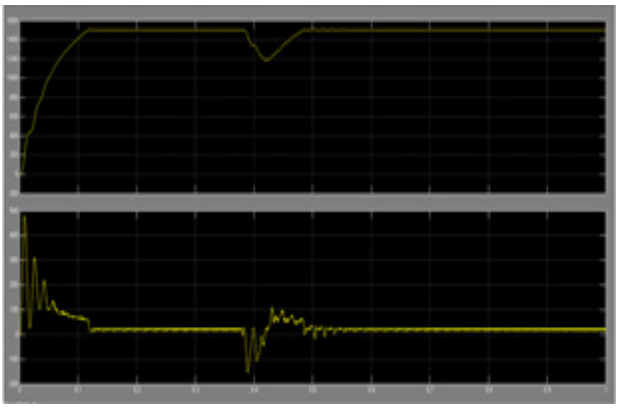

Figure 9. Torque and Speed.

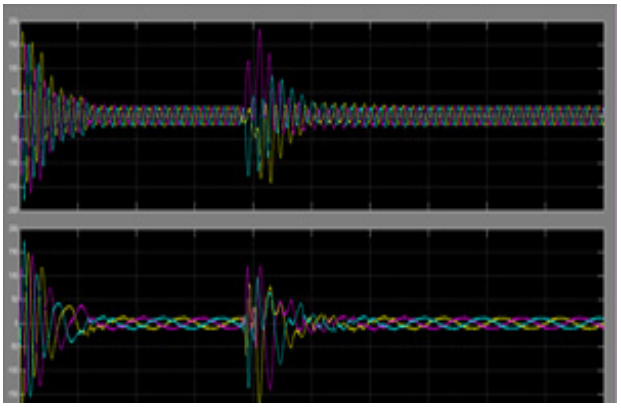

Figure 10. Stator and Rotor currents.

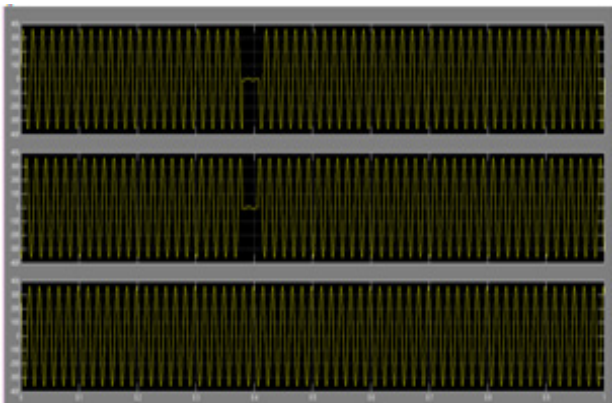

Figure 11. Voltages.

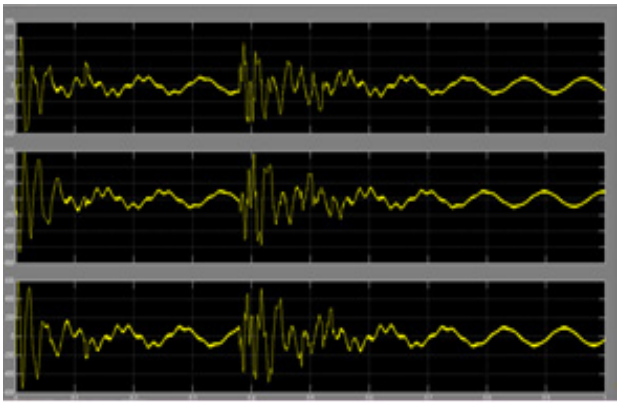

Figure 12. abc to dq transformation.

6. Conclusion

In this paper the low voltage ride through capability with virtual resistance and demagnetizing control was proposed. Demagnetizing control eliminates the stator flux disturbances which results in voltage dip, the resistance and inductances are very low this results demagnetizing current to reach peak value. Crowbars are

neglected used to protect RSC which gets destroyed when high voltages and currents occur at stator and rotor. Here a virtual resistance is implemented to improve control and enhance the LVRT capability. This raises the rotor resistance when fault occurs so that the over currents gets reduced. A virtual resistance with demagnetizing simulation was done on DFIG to meet new grid code requirements. Quick detection of fault is very important in LVRT control strategy.

7. References

1. Lopez J, Sanchis P, R oboam X, Marroyo L. Dynamic behaviour of the doubly-fed induction generator during three-phase voltage dips. IEEE Trans Energy Convers. 2007 Sep; 22(3):709–17.
2. Lopez J, Sanchis P, Gubia E, Ursua A, Marroyo L, Roboam X. Control of doubly fed induction generator under symmetrical voltage dips. Proceeding of International Symposium Ind Electron. U.K: Cambridge; 2008 Jul. p. 2456–62.
3. Zhou P, He Y, Sun D. Improved direct power control of a DFIG-based wind turbine during network unbalance. IEEE Trans Power Electron. 2009 Nov; 24(11):2465–74.
4. Santos-Martin D, Rodriguez-Amenedo JL, Arnaltes S. Providing ride-through capability to a doubly fed induction generator under unbalanced voltage dips. IEEE Trans Power Electron. 2009 Jul; 24(7):1747–57.
5. Kasem AH, El-Saadany EF, El-Tamaly HH, Wahab MAA. A new fault ride-through strategy for doubly fed wind-power induction generator. Proceeding of IEEE Elect Power Conference; Canada; 2007. p. 1–7.
6. Lopez J, Guba E, Sanchis P, Olea E, Ruiz J, Marroyo L. Ride through of wind turbines with doubly fed induction generator under symmetrical voltage dips. IEEE Trans Ind Electron. 2009 Oct; 56(10):4246–54.
7. Lopez J, Guba E, Sanchis P, Roboam X, Marroyo L. Wind turbinesbased on doubly fed induction generator under asymmetrical voltage dips. IEEE Trans Energy Convers. 2008 Mar 23(1): 321–30.
8. Morren J, de Haan SWH. Ride through of wind turbines with doubly-fed induction generator during a voltage dip. IEEE Trans Energy Convers. 2005 June; 20(1):435–41.
9. On E. NetzGmbh. Germany Grid code regulations for high and extra high voltage. Report ENENARHS2006; 2006 Apr 1. p. 46. Available from: www.eon-netz.com
10. Morren J, de Haan SWH. Ride through of wind turbines withdoubly-fed induction generator during a voltage dip. IEEE Trans Energy Convers. 2005 Jun; 20(2): 435–41.
11. Morren J, de Haan SWH. Short-circuit current of wind turbines with doubly fed induction generator. IEEE Trans Energy Convers. 2007 Mar; 22(1):174–80.
12. Zhou L, Liu J, Liu F. Design and implementation of STATCOM combined with series dynamic breaking resistor for low voltage ride through of wind farms. Proceeding of IEEE Energy Convers Congr Expo; 2010 Sep. p. 2501–06.
13. El-Moursi MS, Bak-Jensen B, Abdel-Rahman MH. Novel STATCOM controller for mitigating SSR and damping power system oscillations in a series compensated wind park. IEEE Trans Power Electron. 2010 Feb; 25(2):429–41.
14. Flannery PS, Venkataramanan G. Fault tolerant doubly fed induction generator wind turbine using a parallel grid side rectifier and series grid side converter. IEEE Trans Power Electron. 2008 May; 23(3):1126–35.
15. Yang J, Fletcher JE, O'Reilly J. A series-dynamic-resistor-based converter protection scheme for doubly-fed induction generator during various fault conditions. IEEE Trans Energy Convers. 2010 Jun; 25(2):422–32.
16. Abdel-Baqi O, Nasiri A. A dynamic LVRT solution for doubly fed induction generators. IEEE Trans Power Electron. 2010 Jan; 25(1):193–6.
17. Xiang D, Ran L, Tavner PJ, Yang S. Control of a doubly fed induction generator in a wind turbine during grid fault ride-through. IEEE Trans Energy Convers. 2006 Sep; 21(3):652–62.
18. Lima FKA, Luna A, Rodriguez P, Watanabe EH, Blaabjerg F. Rotor voltage dynamics in the doubly fed induction generator during grid faults. IEEE Trans Power Electron. 2010 Jan; 25(1):118–30.
19. Lopez J, Sanchis P, Roboam X, Marroyo L. Dynamic behaviour of the doubly fed induction generator during three-phase voltage dips. IEEE Trans Energy Convers. 2007 Sep; 22(3):709–17.
20. Lopez J, Sanchis P, Roboam X, Marroyo L. Wind turbine based on doubly fed induction generator under asymmetric voltage dips. IEEE Trans Energy Convers. 2008 June; 23(1):321–30.
21. Yao J, Li H, Liao Y, Chen Z. An improved control strategy of limiting the DC-link voltage fluctuation for a doubly fed induction wind generator. IEEE Trans Power Electron. 2008 May; 3(23):1205–13.
22. Ekanayake JB, Holdsworth L, Wu XG, Jenkins N. Dynamic modeling of doubly fed induction generator wind turbines. IEEE Trans Power Syst. 2003 May; 18(2):803–9.
23. Gomis-Bellmunt O, Junyent-Ferre A, Sumper A, Bergas-Jane J. Ride-through control of a doubly fed induction generator under unbalancedvoltagesags. IEEE Trans Energy Convers. 2008 Dec; 23(4):1036–45.
24. Seman S, Niiranen J, Kanerva S, Arkkio A, Saitz J. Performance study of a double fed wind-power induction generator under network disturbances. IEEE Trans Energy Convers. 2006 Dec; 21(4): 883–90.
25. Rodriguez P, Timbus A, Teodorescu R, Liserre M, Blaabjerg F. Reactive power control for improving wind turbine system behavior under grid faults. IEEE Trans Power Electron. 2009 Jul; 24(7):1798–801.
26. Chen Z, Guerrero JM, Blaabjerg M. A review of the state of the art of power electronics for wind turbines. IEEE Trans Power Electron. 2009 Aug; 24(8):1859–75.
27. Yazdani D, Mojiri M, Bakhshai A, Joos G. A fast and accurate synchronization technique for extraction of symmetrical components. IEEE Trans Power Electron.2009 Mar; 24(3):674–84